

Dynamic Measurements of the Position, Orientation, and DNA Content of Individual Unlabeled Bacteriophages

Aaron M. Goldfain,^{†,||} Rees F. Garmann,^{†,||} Yan Jin,[‡] Yoav Lahini,[¶] and Vinodhan N. Manoharan^{†,¶,*}

[†]Harvard John A. Paulson School of Engineering and Applied Sciences, and

[¶]Department of Physics, Harvard University, Cambridge, MA 02138, USA

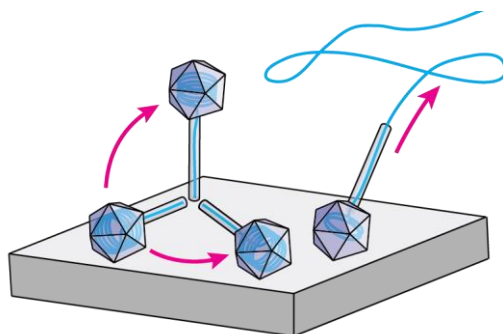
[‡]Department of Chemistry and Biochemistry, University of California, Los Angeles, CA 90095, USA

^{||}These authors contributed equally

*E-mail: ynm@seas.harvard.edu

Abstract

A complete understanding of the cellular pathways involved in viral infections will ultimately require a diverse arsenal of experimental techniques, including methods for tracking individual viruses and their interactions with the host. Here we demonstrate the use of holographic microscopy to track the position, orientation, and DNA content of unlabeled bacteriophages (phages) in solution near a planar, functionalized glass surface. We simultaneously track over 100 individual λ phages at a rate of 100 Hz across a 33 μm x 33 μm portion of the surface. The technique determines the in-plane motion of the phage to nanometer precision, and the height of the phage above the surface to 100-nm precision. Additionally, we track the DNA content of individual phages as they eject their genome following the addition of detergent-solubilized LamB receptor. The technique determines the fraction of DNA remaining in the phage to within 10% of the total 48.5 kilobase pairs. Analysis of the data reveals that under certain conditions, λ phages move along the surface with their heads down and intermittently stick to the surface by their tails, causing them to stand up. Furthermore, we find that in buffer containing high concentrations of both monovalent and divalent salts, λ phages eject their entire DNA in about 7 s. Taken together, these measurements highlight the potential of holographic microscopy to resolve the fast kinetics of the early stages of phage infection.



Introduction

Bacteriophages (phages) are viruses that infect bacteria. Phages come in a variety of morphologies and exploit a range of infection pathways. Here we focus on long-tailed phages with a bulky, hollow protein head that is packed with a high density of double-stranded (ds) DNA and that is connected to a slender, tubular protein tail. In the first stages of infection, the tip of the tail binds a specific protein receptor on the exterior surface of the bacterium, and the phage DNA is ejected from the head through the tail, through the bacterial cell wall, and into the bacterial cytoplasm. While much is known about the specific molecular interactions that underpin tail-receptor binding¹⁻⁵ and the thermodynamic forces that drive DNA ejection⁶⁻⁸, much less is known about the kinetic pathways by which these processes occur. How does the phage navigate the cell surface in order to find and orient itself about its receptor? And how does the densely packed DNA make its way out of the phage head during ejection?

Answering such questions requires resolving the often fast and inherently subtle dynamics of individual phages at the bacterial cell surface. This is a major experimental challenge. To date, fluorescence-based methods have been the only means of probing the kinetics at the single-phage level: fluorescence microscopy and single particle tracking have provided the first glimpses into how fluorescently-labeled phages traverse the exterior surface of the bacterium^{9,10} and how they eject their DNA¹¹⁻¹⁴. However, the full kinetics of these processes remain unresolved, owing to the low measurement rates of standard fluorescence microscopy techniques. The highest frame rates used to track phages thus far have not exceeded a few tens of Hertz, limited by the inherently low emission rates of available fluorophores and the time required to scan a 3D image. Higher temporal resolution is possible with non-fluorescent methods such as elastic scattering, which has recently been used to track individual animal viruses^{15,16} and plant viruses¹⁷. However, elastic scattering methods have not yet been applied to image individual bacteriophages.

Here we apply a label-free imaging method based on holographic microscopy to track the dynamics of a model phage¹⁸ (λ) in solution near a planar glass surface. The method, which has been termed “interferometric scattering” or “iSCAT” by Kukura, Sandoghdar, and coworkers^{15,16,19-23}, records the pattern of interference between light scattered from the phages and the reflection from a nearby coverslip-water interface. This interference pattern is a hologram, and so the technique is similar to other holographic microscopy techniques^{24,25}, except that the weak reflection from the coverslip attenuates the reference wave, improving the fringe intensity relative to the background and making it easier to see weak scatterers such as single phages. Although it is not possible to label and track individual phages in crowded solutions using this technique, it has four key advantages over fluorescence techniques for measurements of dynamics in purified solutions: first, the phages can be detected without the use of chemical or physical labels, eliminating labeling artifacts; second, the intensity of the scattered light depends on the mass of the phage; third, the low-intensity incident light does not damage the sample, so that holograms can be acquired indefinitely; fourth, the measurement speed is much higher. The temporal resolution is limited only by the intensity of the illumination source and the speed of the detector. In our experiments, we can follow over one hundred individual phages in a single frame,

corresponding to a $33\ \mu\text{m} \times 33\ \mu\text{m}$ field of view, and we can capture frames at 100 Hz for tens of minutes. Rates in excess of 1000 Hz are possible for smaller fields of view.

We shall show that the holograms encode not only the position, but also the orientation and DNA content of each phage. From the holograms we track the in-plane motion of phages as they diffuse and stick to the functionalized glass surface. By tracking their out-of-plane motion, we are able to observe the phages spontaneously standing up on their tails. Finally, we demonstrate that the technique can temporally resolve the dynamics of DNA ejection upon addition of detergent solubilized receptor. While the *in vitro* results presented here are indeed far removed from biologically realistic scenarios involving the infection of living bacteria, they demonstrate how holographic microscopy might be used to study the fast kinetics of long-tailed phages interacting with cellular surfaces, orienting about and attaching to membrane receptors, and ejecting their genomic DNA.

Experimental

Growth and purification of phage and receptor: We harvest and purify wild-type λ from infected *E. coli* strain LE392 (Agilent Technologies Inc., Cedar Creek, TX, USA) based on the protocols described by Evilevitch *et al.*⁸ Additionally, we perform a second CsCl density gradient centrifugation step in order to more completely remove impurities that contribute to the background scattering. Following extraction from the second CsCl gradient, we dialyze the purified phage against TNM buffer (50 mM Tris-HCl pH 7.5, 100 mM NaCl, 8 mM MgCl_2) and store the phage solution at 4°C . We use a plaque assay to measure the number of infectious phages; that is, the number that are full of DNA and capable of ejection. We dilute the phage stocks to 10^{12} plaque forming units (pfu) per mL. We use negative-stained transmission electron microscopy to determine that the majority of phages are intact (Figure 1, left).

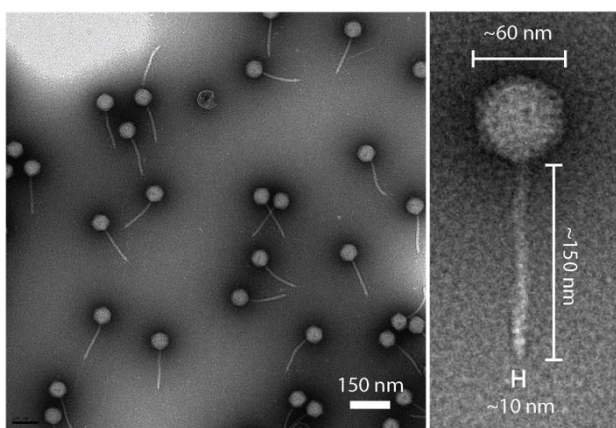


Figure 1: Left: Negative-stained transmission electron micrograph of purified λ phages. Right: Close-up of λ phage with its head and tail dimensions labeled.

We purify LamB receptor from *E. coli* pop154 (provided by Bill Gelbart and Chuck Knobler, UCLA) as described in Evilevitch *et al.*⁸ After purification, we dialyze the LamB against TNM buffer containing 1% n-Octyl-oligo-oxethylene (oPOE) detergent (Enzo Life Sciences Inc., Farmingdale, NY, USA) and store the receptor solution at 4°C. Directly before use, we filter the LamB solution through a sterile 0.2 µm syringe filter (Acrodisc, Low Protein Binding; Pall Life Sciences, Port Washington, NY, USA) to minimize the scattering from aggregates that can form at 4°C.

We prepare DNA-empty phages by equilibrating a few µL of wild-type λ in 100 µL of TNM with 1% oPOE containing LamB at room temperature for 1 h. We perform time-resolved bulk fluorimetry according to the protocols described in Chiaruttini *et al.*²⁶ in order to verify that phages eject their DNA within 1 h: indeed, we observe that the majority of phages eject in less than ten minutes. Following ejection, DNase I (New England Biolabs Inc., Ipswich, MA, USA) is added to digest the ejected DNA.

Glass coverslip functionalization: We modify the glass coverslips based on the protocols described in Joo and Ha²⁷. For tracking measurements we functionalize the glass with 3-Aminopropyltriethoxysilane (APTES) (98% purity; Alfa Aesar, Ward Hill, MA, USA) in order to generate an electrostatic attraction between the positively charged APTES surface and the negatively charged phage²⁸. For DNA ejection measurements we react the APTES-coated coverslips with 5,000 MW polyethylene glycol (PEG) that is functionalized at one end with an N-hydroxylsuccinimide (NHS) group (>95% purity, used as received; Nanocs Inc., NY, USA). To favor lower densities of surface grafted PEG, we modify the protocol of Joo and Ha²⁷ to reduce the amount of PEG by a factor of 100 to 1,000. The patchy layer of covalently grafted PEG limits the number of phages that bind to a given area of the APTES-coated surface and also restricts the motion of the bound phages.

The microscope: The reflection-mode holographic microscope sketched in Figure 2A is based on the iSCAT microscope first described by Jacobsen *et al.*¹⁹ with polarization optics to minimize losses at the beam splitter²². A laser (Toptica iBeam Smart, 300 mW, wavelength $\lambda = 405$ nm) is coupled into a single mode optical fiber and focused into the back aperture of an infinity-corrected oil immersion objective (Nikon PlanApo VC, 100×, NA=1.4) to produce a collimated beam (intensity $I_i \sim 10$ W/cm²) with diameter ~ 100 µm illuminating the sample chamber. A fraction ($R \sim 0.004$) of the illuminating beam is reflected at the bottom of the sample chamber by the coverslip-water interface. The sample chamber is designed so that reflections from the top of the chamber do not re-enter the objective (see *Loading the sample*). The reflected beam serves as the reference wave for the hologram. The reference beam (intensity I_r) and the light scattered from the virus (intensity I_s) are collected by the objective, and the resulting hologram is imaged onto a camera (Andor Zyla 5.5) with 100× total magnification, yielding an effective pixel size of 65 nm.

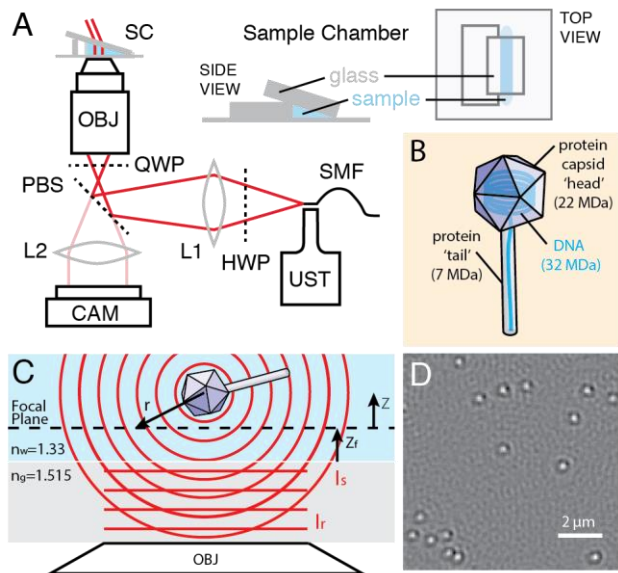


Figure 2. A: Schematic of the reflection mode holographic microscope and sample chamber. SMF = single mode optical fiber, UST = ultrasonic transducer, HWP = half wave plate, L1 = lens, PBS = polarizing beam splitter, QWP = quarter wave plate, OBJ = Objective, SC = sample chamber, L2 = tube lens, CAM = camera. **B:** Our optical model of phage λ assumes that its polarizability is directly proportional to the total mass of the phage head including DNA, as described by Rajagopala *et al.*²⁹ **C:** Cartoon of our hologram model for λ phage, n_w = water refractive index, n_g = glass refractive index, r = distance from head center to a point in focal plane, z = height of head center above focal plane, z_f = distance from coverslip to focal plane, I_r = reference beam intensity, I_s = scattered light intensity. **D:** Background divided hologram (10-frame average) of λ phages bound to an APTES-PEG functionalized coverslip recorded with a 6.2 ms exposure.

A major challenge of using wide-field coherent illumination is reducing spatial variations in the intensity of the reference beam caused by interference fringes from dust particles, scratches, and inherent imperfections in the optical components. To eliminate back reflections from the objective we slightly tilt and displace the incident beam, which moves these reflections out of the field of view and makes the holograms slightly asymmetric. We smooth out some of the remaining spatial intensity variations by reducing the temporal coherence of the laser. We do this by pulsing the current to the laser diode at 1 MHz with a 50% duty cycle. Pulsing the current with a period shorter than the exposure time of the camera reduces the temporal coherence because the wavelength shifts slightly when the current changes³⁰. We further reduce the variations by oscillating the illuminating beam at frequencies larger than the inverse exposure time; we do this by epoxying the end of the optical fiber to an ultrasonic transducer and horn (Figure 2A; built in-house) that mechanically oscillate the end of the fiber by tens

of micrometers at 20 kHz. The resulting reflected beam is significantly more uniform than the stationary beam. We digitally remove the remaining spatial variations in the reflected beam as described below (see *Image processing and data analysis*).

Loading the sample: We construct a special sample chamber to facilitate buffer exchange and minimize unwanted reflections. As shown in Figure 2A, the sample chambers have a “lean-to” design. Each chamber consists of a single No. 1 glass coverslip and two rectangular strips of a glass slide (thickness = 1 mm) cut with a glass scorer. The coverglass serves as the floor of the sample chamber, and one of the strips of glass serves as the tilted roof that rests along its long edge on the second strip of glass. The internal volume of each chamber is approximately 20 μL . All of the glass-glass contacts are sealed with vacuum grease (Dow Corning, High vacuum grease). The ends are left open.

All experiments are carried out at room temperature. We introduce phage into the sample chamber by pipetting a 20 μL aliquot of 10^{10} pfu per mL of λ -phage in TNM buffer into one end of the sample chamber. After a few minutes, we flush any phages that are not adsorbed to the coverslip out of the sample chamber by depositing a 20 μL aliquot of TNM at one end of the chamber and aspirating an equal volume from the other end. A similar flushing procedure is used to introduce TNM with 1% oPOE detergent or TNM with 1% oPOE detergent and receptor LamB.

Recording holograms: Time-series of holograms are typically recorded with a frame rate of 100 Hz and an exposure time of about 6 ms. We use a total field of view of $33 \mu\text{m} \times 33 \mu\text{m}$ to simultaneously track hundreds of phages. Higher frame rates (over 1,000 Hz) can be obtained with a narrower illumination beam and a smaller field of view. Background images, representing the reference beam intensity and any scattering that arises from imperfections along the optical path, are obtained by taking the time median of 10-4,000 frames when the phages are either not present or while they are moving distances larger than the spacing between hologram fringes. We set the focal plane of the microscope slightly below the coverslip so that the coverslip is still in focus. In this configuration, the central fringe of the holograms has its maximum intensity when the head is adsorbed to the coverslip.

Image processing and data analysis: All of our image processing and data analysis operations are carried out using the Python programming language with Numpy³¹ and Scipy³² extensions. After obtaining the raw data, we reduce the fringe noise by using a spatial bandpass filter (Fourier radial step filter, keeping features of size 0.5-5 pixels) on the raw holograms and then dividing them by a background image with no phage present. The remaining noise in the image is primarily shot noise (root mean square intensity of 0.006 relative to background). When a higher signal-to-noise ratio is desired we decrease the shot noise intensity by averaging subsequent frames.

To track phages in-plane, we identify the center of the bright central fringe of the hologram by fitting it to a 2D Gaussian using the software package TrackPy³³. We estimate the positioning uncertainty using fixed phages, as described in *Phage Motion*. To track the out-of-plane motion of the phage, we use the Hough-

transform method³⁴ implemented in the software package HoloPy³⁵ to locate the center of the ring pattern recorded in each frame.

Interpreting the holograms and extracting information about the position and mass of individual phages requires a model of hologram formation (Figures 2B and 2C). We model phage λ as a Rayleigh scatterer with its center coincident with the center of the phage head. We assume that the tail does not contribute significantly to the scattering. These approximations are supported by the observations that the diameter of the head is much smaller than the wavelength of the scattered light and that the head contains roughly 90 percent of the total mass of the phage. We take the mass of the DNA in the head to be 32 MDa, the total mass of protein in the head to be 22 MDa, and the total mass of protein in the tail to be 7 MDa (Figure 2B), based on the protein interaction map described in Rajagopala *et al.*²⁹

The circular fringes of the hologram recorded by the camera (Figure 2D) can be described as $I = I_r + I_s + 2\sqrt{I_r I_s} \cos \varphi$ where $I_r = R I_i$ and φ is the phase difference between the planar reflected wavefronts and spherical scattered wavefronts^{15,16,19–23}. After background division we obtain the normalized hologram $H = I/I_r \approx 1 + 2\sqrt{I_s/I_r} \cos \varphi$, where we have dropped the scattered intensity term, which is negligible compared to the interference term. For our model of phage λ as a Rayleigh scatterer³⁶, $I_s = I_i \frac{\pi^2}{2(\lambda/n_w)^4} \frac{\alpha^2}{r^2}$ and $\varphi = k(r + z + z_f)$, where α is the total polarizability of the phage head, z the height of the phage above the focal plane, z_f the distance from the focal plane to the water-coverslip interface, $r = \sqrt{x^2 + y^2 + z^2}$ the distance from the phage to a given point in the focal plane, and $k = 2\pi n_w/\lambda$. The resulting normalized hologram is

$$H \approx 1 + \frac{\pi\sqrt{2/R}}{(\lambda/n_w)^2} \frac{\alpha}{r} \cos\left(k(r + z + z_f)\right) \quad (1)$$

where we have assumed that the objective and tube lens simply relay the magnified hologram to the camera^{24,25,37}.

Equation (1) shows how a single hologram, which records both the phase and the intensity of light scattered from the sample^{21,24,25,37}, encodes the 3D position and the DNA content of unlabeled phage. The DNA content can be inferred from the total polarizability (α), which depends on the mass of the capsid and the mass of the DNA³⁶. We measure the relationship between α and the DNA content of the phage in *DNA ejection*, below. Thus, the 3D position and DNA content can be sampled at rates limited only by the illumination intensity and frame rate of the camera.

Most non-interferometric scattering methods cannot detect phages because the intensity of the scattered light scales as the square of the polarizability α , which is small. Such weak scattering is difficult to detect unless the background is extremely uniform¹⁷. In interferometric methods such as holography, the signal intensity relative to the reference beam intensity scales linearly with α , making it easier to detect weak scatterers.

The normalized intensity of a reflection-mode hologram is further enhanced because the reference wave is attenuated relative to the incident beam, owing to the low-intensity reflection from the coverslip-water interface. The attenuation of the reference beam ensures that shot noise does not overwhelm the interference fringes

of the phage. Furthermore, the fringes of reflection-mode holograms invert when the scatterer moves in the axial (z) direction by just a quarter of the illumination wavelength in medium (76 nm), as seen from the cosine term of Equation (1). The strong dependence of fringe intensity on z gives rise to the excellent axial precision previously reported with reflection-mode holographic microscopes^{21,37}. Below, we describe how we use our model of the phage hologram to infer the orientation and DNA content of the phage.

Results and Discussion

Phage motion

First we examine the motion of individual λ phages near functionalized glass surfaces. Recent single-particle tracking measurements^{9,10} of fluorescently labeled λ phages in solution with living *E. coli* have revealed both reversible and irreversible binding between the tail of the phage and the anisotropic distribution of LamB receptors that populate the bacterial surface. These measurements have raised a number of questions concerning the fast kinetics of both specific binding (interactions between the tip of the tail of the phage and the cellular receptor) and non-specific binding (between any part of the phage and any portion the cell surface) and the related problem of how phages identify and orient about the final ejection site. While the surfaces we feature are not biological, the recorded tracks demonstrate that a surprisingly rich variety of phage-surface interactions can be resolved on short timescales.

The types of interactions we observe depend on both the surface functionalization and the buffer conditions. On non-functionalized glass that was cleaned either by heating in Alconox detergent¹² or by pyrolysis (PYRO-CLEAN, Tempyrox Co.) followed by sonication in ultrapure water for 30 min, we find that phages in TNM buffer are bound to the glass but not completely immobilized. We infer the motion of the phages from the recorded holograms, which show fluctuating fringe patterns (see Supporting Information, Video S1). We interpret these fluctuations as arising from motion of the head of the phage perpendicular to the surface on time scales shorter than our 1 ms exposure time. We attribute this perpendicular motion to phages that are adsorbed to the glass only by their tails, with their heads subject to thermal motion above the surface. This interpretation is discussed in more detail at the end of this section.

To obtain higher quality holograms, we functionalize the coverglass with APTES to produce an electrostatic attraction between the negatively charged phage²⁸ and the positively charged APTES surface. On APTES-functionalized glass we find that phages in TNM buffer produce holograms with stable fringe intensity. However, the fringes typically translate between frames (Figure 3, left; Video S2), consistent with phages moving slowly across the APTES surface with their heads down. Addition of 1% oPOE detergent to the TNM buffer solution increases the general mobility of the phages (Figure 3, right; Video S3) as well as the frequency of large displacements between frames. In addition to the large numbers of mobile phages, we also observe a few phages that appear to be immobilized on the surface. We quantify our tracking precision by measuring the standard deviation of the tracked positions of an immobilized phage³⁸. The tracking precision is 5.6 nm

with a standard deviation of 1.4 nm for holograms recorded at 100 Hz with a 6.5 ms exposure time.

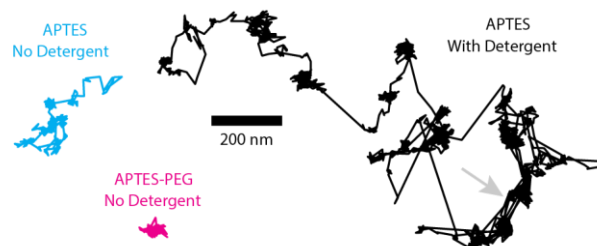


Figure 3: Representative in-plane tracks of phages moving along coverslips with different functionalizations in different buffer solutions. 34.7 seconds of each track is shown. When there is no detergent in the buffer the holograms are recorded at 10 Hz with a 28 ms exposure (Videos S2-S3). When there is detergent the frame rate is 100 Hz with a 6.5 ms exposure (Video S4). The gray arrow points to a circular portion of the track.

For phages on APTES-functionalized glass in TNM with 1% detergent, about half of the tracks have segments that are constrained along the perimeter of a circle (see the portion of the track indicated by a gray arrow in Figure 3; also, see the last 15 s of Video S3). In some cases the circular track lasts many tens of seconds, and in each case the radius is roughly 180 nm. For example, Figure 4A (Video S5) shows a circular track with a radius of 180 ± 12 nm. We therefore infer that these tracks represent the head of the phages diffusing in a circle with the tip of the tail immobilized at a point, as illustrated in Figure 4B, arrow (2). The 180-nm radius of the circular tracks is consistent with the coarse structural model of phage λ where the head diameter measures between 60-70 nm (depending on orientation of the facets) and the tail length is between 150-165 nm (depending on the fine structure of the tip). Additionally, the agreement between the radius of the circular tracks and the distance of the head from the tip of the tail validates our optical model of the phage as a Rayleigh scatterer positioned at the center of the head. However, the width of the distribution of measured radii is larger than the tracking precision, which might reflect the flexibility of the tail or indicate that the tip of the tail is moving slightly across the surface. The observation that certain tracks show segments of circular motion in between segments of random unconfined motion (illustrated in Figure 4B (1)) demonstrates that tail binding is reversible.

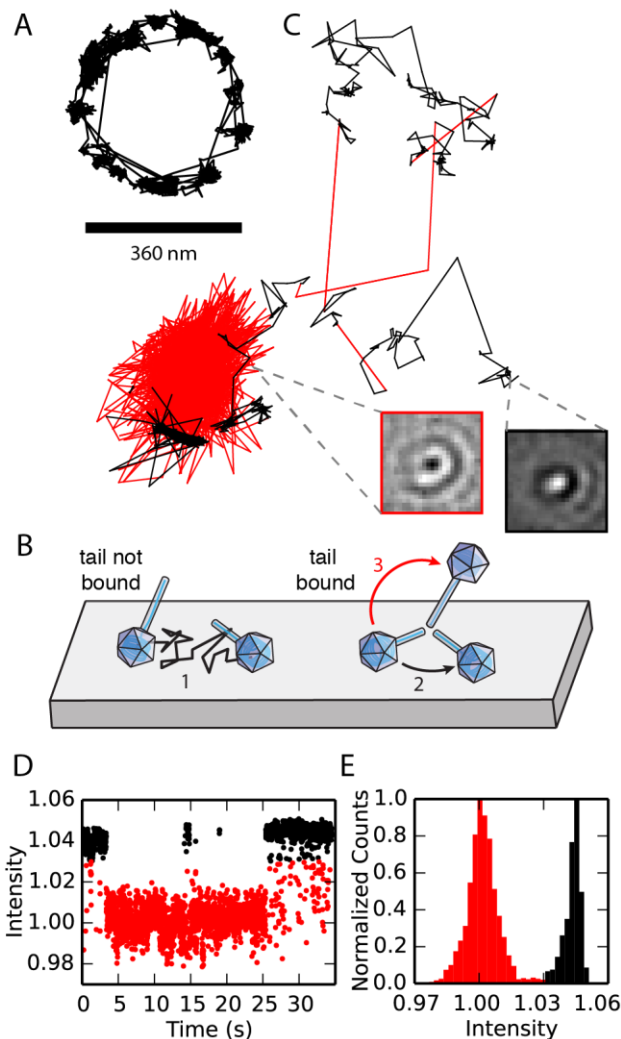


Figure 4: Tracking λ phages on APTES-functionalized coverglass in TNM buffer with detergent. Videos were recorded at 100 Hz with a 6.5 ms exposure. **A:** 40.95 second in-plane circular track of a phage with the tip of its tail adsorbed to the coverslip (Video S5). **B:** Illustration of a phage (1) moving parallel to the surface with its head down and its tail not bound, (2) moving with its head down and the tip of its tail fixed at a single point, (3) standing up on its tail. **C:** 34.53 second track (Video S6) of a phage moving with its head on (black) and off (red) the coverslip. Insets show holograms when the phage is on and off the coverslip. A phage is determined to be off the coverslip when its normalized central fringe intensity is below 1.03, as determined from **D:** The normalized central fringe intensity of the hologram at each frame of the video. **E:** Histograms of the normalized central fringe intensity when the phage head is on (black) and off (red) the coverslip.

We also find that phages occasionally stand up on their tails (illustrated in Figure 4B arrow (3)) on APTES-functionalized glass in TNM with 1% detergent. Figure 4C shows the track of such a phage (Video S6). For the first 4 s of the track, the phage traverses the coverslip with its head mostly on the surface (black track) and its tail not bound. During this time the normalized central fringe intensity, which is measured by averaging the intensity within a 100-nm radius of the center of the normalized hologram, is 1.043 with a standard deviation of 0.004 (Figures 4D and 4E, black). For the next 30 s, the phage remains within a 180-nm radius. During most of this 30 s window, the phage hologram has a darker center and the fringe pattern is blurred (red track): the normalized central fringe intensity is 1.002 with a standard deviation of 0.007 (Figures 4D and 4E, red). A dark center fringe indicates that the phage head is above the coverslip (see *Image processing and data analysis*), and a broad distribution of the normalized central fringe intensities in time suggests movement perpendicular to the coverslip. The blurring of the hologram further suggests that the perpendicular movement occurs on time scales shorter than the exposure time. Taken together, these observations are consistent with the phage standing up. While standing, the head is shuffled about by thermal motion above the coverslip and the tail is fixed at a single point on the surface.

We note that the in-plane tracking precision is significantly degraded for phages that are standing up because the holograms are blurred. We are not able to quantify the tracking precision for standing phages by measuring the standard deviation in the position of an immobilized phage, as is done for phages with their heads on the surface, since standing phages are continually moving. Instead, we estimate the tracking precision by locating the center of the hologram by eye and measuring the distance from the center to the tracked position. In this way we estimate the upper bound on the tracking precision to be 100 nm.

Returning to the case of the bare glass coverslip, we conclude that the majority of the phages are standing up with their tails bound securely to the glass. This observation is consistent with the presence of electrostatic repulsions between the head of the phage and the coverglass, which are both expected to bear negative surface charges at neutral pH. Furthermore, the observation that the heads of phages bind readily to the positively charged APTES-functionalized coverslip suggests that electrostatics might play a significant role in how phages attach to surfaces, but additional experiments in which the ionic strength of the buffer is varied are necessary to test this hypothesis.

The observed dynamics demonstrate that holographic microscopy can be used to measure the orientation of phages on a surface at biologically relevant timescales. Information about the orientation allows us to distinguish tail-surface binding from head-surface binding and unbinding, and thus enables measurements of the kinetics of phage adsorption in the presence of specific and non-specific interactions. Performing similar experiments with a supported lipopolysaccharide bilayer containing the appropriate receptor proteins that mimics the outer membrane of gram negative bacteria may further elucidate the target-finding mechanisms that precede irreversible binding and DNA ejection for a variety of different long-tailed phages.

DNA ejection

Here we demonstrate that holographic microscopy can be used to resolve the dynamics of DNA ejection from individual phages. The kinetics of DNA ejection has been the subject of a number of theoretical^{39,40} and computational^{41–44} studies, and has been treated experimentally both *in vitro*^{12,13} and *in vivo*^{14,45}. In general, ejection of the initial portion of DNA from the phage into the bacterium is driven by the internal stress associated with the dense packing of DNA in the capsid^{39,46,47}. DNA ejection from certain phages into bulk solution can be triggered spontaneously by the addition of receptor that is made soluble by incorporating it into detergent micelles. This *in vitro* ejection process has been the subject of a number of bulk^{4,5,8,48–50} and single-molecule^{11–14,51–54} studies. Most recently, single-molecule fluorescence microscopy^{12,13} was used to measure the timescale for the DNA to translocate from the capsid of phage λ into solution: it was found that the DNA ejects completely and continuously in 1 to 10 s, depending on the concentrations of monovalent (Na^+) and divalent (Mg^{2+}) ions in solution.

The smooth ejection profile previously measured for phage λ ^{12,13} is distinct from that of phage T5^{4,11} which ejects its DNA in a number of bursts separated by long pauses that are thought to be associated with the reconfiguration of the DNA inside the capsid⁵⁴. It is not currently known why such long pauses are not seen for phage λ . However, it is possible that smaller fluctuations in the rate of ejection may be present but not resolved by the low (4 Hz) frame rates of the previous measurements.

We resolve the kinetics of DNA ejection with higher (100 Hz) time resolution by measuring the decrease in the intensity of the phage hologram that occurs as DNA exits the capsid. To characterize the reduction in intensity following ejection, we record holograms of DNA-full and DNA-empty phages in the same sample chamber (see *Growth and purification of phage and receptor*). The two types of phages are readily distinguished (Figure 5A). We measure the normalized central fringe intensity of 10 holograms of 10 different DNA-full phages and find a mean value of 1.035 with a standard error of 0.002 (Figure 5B). We perform a similar measurement on DNA-empty phages (mass relative to full phage of 0.41) and find a mean value of 1.014 with a standard error of 0.001 (Figure 5B). A plot of these values, along with the normalized intensity over a comparable area of the coverslip without any phage (relative mass 0.0), reveals a linear relationship between the normalized central fringe intensity and the relative mass of the phage head. We also compare line scans (Figure S1) of the holograms of full and empty phages and find that the scans are consistent with the same linear relationship. While fully determining the relationship between the central fringe intensity and the total mass of the head will require additional measurements of phages containing varying amounts of DNA, we assume here that the two are directly proportional because this is the simplest model that is consistent with the data. This assumption implies that the polarizability per mass of the capsid is roughly equal to that of the DNA, in contrast to the results of previous bulk light scattering measurements by de Frutos *et al.*⁴ on a different phage (T5) using 633 nm light.

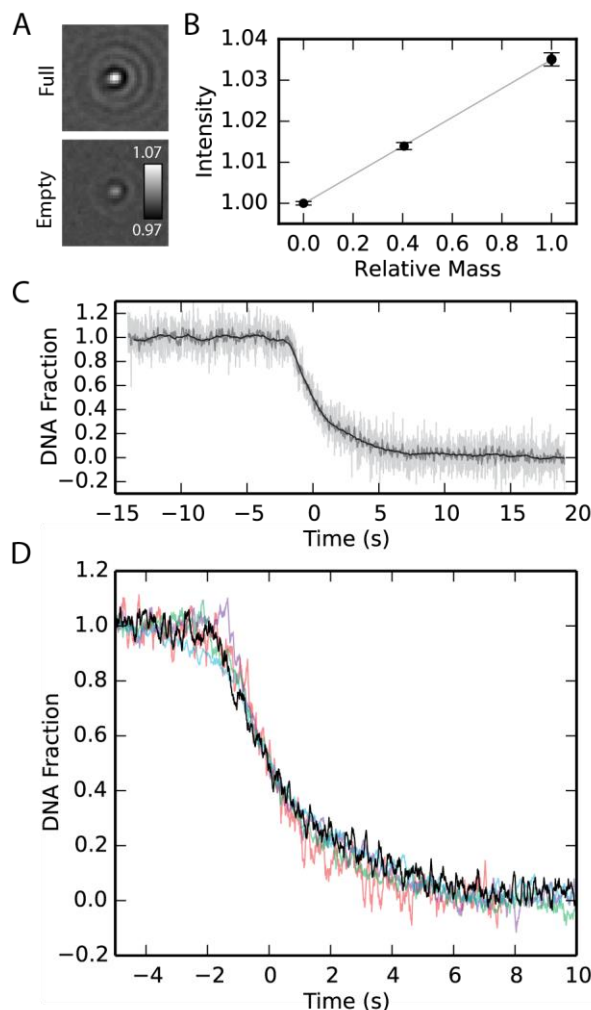


Figure 5: Phages stuck securely to a APTES-PEG functionalized coverslip eject their DNA upon interaction with the receptor protein LamB. Holograms are recorded at 100 Hz with an exposure time of 6 ms. **A:** 10-frame averaged holograms of phages before (top) and after (bottom) ejecting their DNA. The normalized intensity is indicated in the legend in the lower hologram. See Figure S1 for line scans of these holograms. **B:** The normalized central fringe intensity of full phages, ejected phages, and no phages as a function of the mass of the head relative to that of the full phage. Error bars represent the standard error on the mean. **C:** The fraction of DNA in the capsid during one ejection event is plotted in light gray. The dark gray curve is a 10-frame moving average of the data. The black curve is a 100-frame moving average. **D:** The fraction of DNA in the capsid during five separate ejections using a 10-frame moving average. The black curve corresponds to the data in Figure 5C.

Because motion of the phages on the coverslip makes measurement of the normalized central fringe intensity difficult, we increase the fraction of immobile phages by partially passivating the APTES surface with an incomplete coating of covalently bound PEG; our interpretation is that phages can adsorb to sparse defects in the PEG layer but cannot explore the neighboring PEG-coated surface (Figure 3, bottom; Video S4).

We image the dynamics of DNA ejection by first flowing TNM buffer with detergent solubilized LamB over the phages and then recording holograms at 100 Hz for tens of minutes. We observe a small number of phage holograms whose normalized central fringe intensities smoothly decrease by an amount corresponding to the difference between DNA-full and DNA-empty phages. The observed decreases in intensity occur over approximately 7 s, a timescale consistent with that obtained in previous studies^{12,13} performed under different concentrations of Na⁺ and Mg²⁺ ions. Furthermore, we do not observe any such events in the absence of LamB, leading us to conclude that the changes in intensity are indeed due to DNA ejections.

Only a few percent of the phages that are bound to the surface eject their DNA within 30 minutes of adding LamB. However, in bulk, the majority of phages eject within the first ten minutes under identical solution conditions (see *Growth and purification of phage and receptor*). While we did not directly investigate the cause of this discrepancy, it is possible that the tail-surface interactions that we describe above (see *Phage motion*) interfere with the initiation of ejection.

We quantify the amount of DNA remaining in the phage as a function of time by exploiting the proportionality between the normalized central fringe intensity and the number of DNA base pairs remaining in the capsid. We show in Figure S1 that the ejected DNA outside of the phage does not generate appreciable scattering, as was previously shown by de Frutos *et al.*⁴ Figure 5C shows the inferred DNA content as a function of time for one ejecting phage. The vertical axis is linearly scaled so that the time-averaged value of the normalized central fringe intensity of the phage hologram before ejection corresponds to a DNA-fraction of 1, and the time-averaged intensity after ejection corresponds to a DNA-fraction of 0. The main contribution to the noise in our holograms is shot noise and, when averaged over the area of the central fringe, the root mean square shot noise intensity is 0.002. Given that the difference in intensity between DNA-full and DNA-empty phages is 0.021 (Figure 5B) and the length of the DNA is 48.5 kbp, the shot noise contributes a measurement uncertainty of 4.2 kbp per frame. The shot noise intensity can be diminished by averaging subsequent frames (Figure 5C), giving a measurement uncertainty of 1.3 kbp with a ten frame average, and 0.4 kbp with a 100 frame average.

We repeat the experiment in order to record many tens of ejection events, five of which are plotted in Figure 5D. The curves are offset horizontally so that they all overlap at the point where half of the DNA remains in the capsid. The similarity between the separate curves confirms that they are representative of the same general ejection process. Determining whether there are fine-scale fluctuations in the instantaneous rate of ejection, or significant differences between the shapes of the curves that might reflect the presence of non-equilibrated conformations of the packed DNA^{54–57} will be the focus of future work.

Conclusions

Ultimately, a combination of complementary time-resolved techniques will be required to fully address some of the longstanding questions about the early stages of the bacteriophage life cycle. Here we have demonstrated that holographic microscopy may be able to help address such questions. We have shown that the technique can be used to infer—with high temporal resolution (100 Hz) and long duration (tens of minutes)—the position and orientation of many unlabeled λ phages interacting with a surface. The technique is capable of localizing the in-plane position of mobile phages to a precision of about 5 nm. The precision of out-of-plane measurements is sufficient to infer the head-tail orientation of the phage with respect to the surface. In addition, the technique can be used to measure the DNA content of immobilized phages and to resolve the kinetics of DNA ejection with a precision of 4.2 kpb per frame.

Supporting Information

Line scans of holograms of full and empty phages and movies of holograms of phages interacting with different functionalized surfaces are supplied as Supporting Information.

Acknowledgments

We thank Marek Piliarik and Vahid Sandoghdar for helpful discussions about iSCAT microscopy. This work was supported in part by the Harvard MRSEC, supported by the National Science Foundation under award no. DMR-1420570. It was performed in part at the Center for Nanoscale Systems (CNS), a member of the National Nanotechnology Coordinated Infrastructure Network (NNCI), which is supported by the National Science Foundation under NSF award no. 1541959. CNS is part of Harvard University. Additionally, this material is based upon work supported in part by the National Science Foundation Graduate Research Fellowship under award no. DGE-1144152.

References

- (1) Randall-Hazelbauer, L.; Schwartz, M. Isolation of the Bacteriophage Lambda Receptor from Escherichia Coli. *J. Bacteriol.* **1973**, *116*, 1436–1446.
- (2) Werts, C.; Michel, V.; Hofnung, M.; Charbit, A. Adsorption of Bacteriophage Lambda on the LamB Protein of Escherichia Coli K-12: Point Mutations in Gene J of Lambda Responsible for Extended Host Range. *J. Bacteriol.* **1994**, *176*, 941–947.
- (3) Wang, J.; Hofnung, M.; Charbit, A. The C-Terminal Portion of the Tail Fiber Protein of Bacteriophage Lambda Is Responsible for Binding to LamB, Its Receptor at the Surface of Escherichia Coli K-12. *J. Bacteriol.* **2000**, *182*, 508–512.
- (4) de Frutos, M.; Letellier, L.; Raspaud, E. DNA Ejection from Bacteriophage T5: Analysis of the Kinetics and Energetics. *Biophys. J.* **2005**, *88*, 1364–1370.

- (5) Raspaud, E.; Forth, T.; São-José, C.; Tavares, P.; de Frutos, M. A Kinetic Analysis of DNA Ejection from Tailed Phages Revealing the Prerequisite Activation Energy. *Biophys. J.* **2007**, *93*, 3999–4005.
- (6) Kindt, J.; Tzlil, S.; Ben-Shaul, A.; Gelbart, W. M. DNA Packaging and Ejection Forces in Bacteriophage. *Proc. Natl. Acad. Sci.* **2001**, *98*, 13671–13674.
- (7) Tzlil, S.; Kindt, J. T.; Gelbart, W. M.; Ben-Shaul, A. Forces and Pressures in DNA Packaging and Release from Viral Capsids. *Biophys. J.* **2003**, *84*, 1616–1627.
- (8) Evilevitch, A.; Lavelle, L.; Knobler, C. M.; Raspaud, E.; Gelbart, W. M. Osmotic Pressure Inhibition of DNA Ejection from Phage. *Proc. Natl. Acad. Sci.* **2003**, *100*, 9292–9295.
- (9) Rothenberg, E.; Sepúlveda, L. A.; Skinner, S. O.; Zeng, L.; Selvin, P. R.; Golding, I. Single-Virus Tracking Reveals a Spatial Receptor-Dependent Search Mechanism. *Biophys. J.* **2011**, *100*, 2875–2882.
- (10) Chatterjee, S.; Rothenberg, E. Interaction of Bacteriophage λ with Its E. Coli Receptor, LamB. *Viruses* **2012**, *4*, 3162–3178.
- (11) Mangenot, S.; Hochrein, M.; Rädler, J.; Letellier, L. Real-Time Imaging of DNA Ejection from Single Phage Particles. *Curr. Biol.* **2005**, *15*, 430–435.
- (12) Grayson, P.; Han, L.; Winther, T.; Phillips, R. Real-Time Observations of Single Bacteriophage λ DNA Ejections in Vitro. *Proc. Natl. Acad. Sci.* **2007**, *104*, 14652–14657.
- (13) Wu, D.; Van Valen, D.; Hu, Q.; Phillips, R. Ion-Dependent Dynamics of DNA Ejections for Bacteriophage λ . *Biophys. J.* **2010**, *99*, 1101–1109.
- (14) Van Valen, D.; Wu, D.; Chen, Y.-J.; Tuson, H.; Wiggins, P.; Phillips, R. A Single-Molecule Hershey-Chase Experiment. *Curr. Biol.* **2012**, *22*, 1339–1343.
- (15) Ewers, H.; Jacobsen, V.; Klotzsch, E.; Smith, A. E.; Helenius, A.; Sandoghdar, V. Label-Free Optical Detection and Tracking of Single Virions Bound to Their Receptors in Supported Membrane Bilayers. *Nano Lett.* **2007**, *7*, 2263–2266.
- (16) Kukura, P.; Ewers, H.; Müller, C.; Renn, A.; Helenius, A.; Sandoghdar, V. High-Speed Nanoscopic Tracking of the Position and Orientation of a Single Virus. *Nat. Methods* **2009**, *6*, 923–927.
- (17) Faez, S.; Lahini, Y.; Weidlich, S.; Garmann, R. F.; Wondraczek, K.; Zeisberger, M.; Schmidt, M. A.; Orrit, M.; Manoharan, V. N. Fast, Label-Free Tracking of Single Viruses and Weakly Scattering Nanoparticles in a Nanofluidic Optical Fiber. *ACS Nano* **2015**, *9*, 12349–12357.
- (18) Casjens, S. R.; Hendrix, R. W. Bacteriophage Lambda: Early Pioneer and Still Relevant. *Virology* **2015**, *479–480*, 310–330.
- (19) Jacobsen, V.; Stoller, P.; Brunner, C.; Vogel, V.; Sandoghdar, V. Interferometric Optical Detection and Tracking of Very Small Gold Nanoparticles at a Water-Glass Interface. *Opt. Express* **2006**, *14*, 405–414.

- (20) Ortega-Arroyo, J.; Kukura, P. Interferometric Scattering Microscopy (iSCAT): New Frontiers in Ultrafast and Ultrasensitive Optical Microscopy. *Phys. Chem. Chem. Phys.* **2012**, *14*, 15625–15636.
- (21) Mojarad, N.; Sandoghdar, V.; Krishnan, M. Measuring Three-Dimensional Interaction Potentials Using Optical Interference. *Opt. Express* **2013**, *21*, 9377–9389.
- (22) Ortega Arroyo, J.; Andrecka, J.; Spillane, K. M.; Billington, N.; Takagi, Y.; Sellers, J. R.; Kukura, P. Label-Free, All-Optical Detection, Imaging, and Tracking of a Single Protein. *Nano Lett.* **2014**, *14*, 2065–2070.
- (23) Piliarik, M.; Sandoghdar, V. Direct Optical Sensing of Single Unlabelled Proteins and Super-Resolution Imaging of Their Binding Sites. *Nat. Commun.* **2014**, *5*, 4495.
- (24) Lee, S.-H.; Roichman, Y.; Yi, G.-R.; Kim, S.-H.; Yang, S.-M.; van Blaaderen, A.; van Oostrum, P.; Grier, D. G. Characterizing and Tracking Single Colloidal Particles with Video Holographic Microscopy. *Opt. Express* **2007**, *15*, 18275–18282.
- (25) Kaz, D. M.; McGorty, R.; Mani, M.; Brenner, M. P.; Manoharan, V. N. Physical Ageing of the Contact Line on Colloidal Particles at Liquid Interfaces. *Nat. Mater.* **2012**, *11*, 138–142.
- (26) Chiaruttini, N.; de Frutos, M.; Augarde, E.; Boulanger, P.; Letellier, L.; Viasnoff, V. Is the In Vitro Ejection of Bacteriophage DNA Quasistatic? A Bulk to Single Virus Study. *Biophys. J.* **2010**, *99*, 447–455.
- (27) Joo, C.; Ha, T. Single-Molecule FRET with Total Internal Reflection Microscopy. *Cold Spring Harb. Protoc.* **2012**.
- (28) Penrod, S. L.; Olson, T. M.; Grant, S. B. Whole Particle Microelectrophoresis for Small Viruses. *J. Colloid Interface Sci.* **1995**, *173*, 521–523.
- (29) Rajagopala, S. V.; Casjens, S.; Uetz, P. The Protein Interaction Map of Bacteriophage Lambda. *BMC Microbiol.* **2011**, *11*, 213.
- (30) Dulin, D.; Barland, S.; Hachair, X.; Pedaci, F. Efficient Illumination for Microsecond Tracking Microscopy. *PLoS ONE* **2014**, *9*, e107335.
- (31) Ascher, D.; Dubois, P. F.; Hinsen, K.; Hugunin, J.; Oliphant, T. Numerical Python, Tech. Report UCRL-MA-128569. Lawrence Livermore National Laboratory. 2001. www.numpy.org (accessed April, 7 2016)
- (32) Jones, E.; Oliphant, T.; Peterson, P. SciPy: Open source scientific tools for Python. 2001. www.scipy.org (accessed April, 7 2016)
- (33) Allan, D.; Uieda, L.; Boulogne, F.; Perry, R. W.; Caswell, T. A.; Keim, N. Trackpy: Trackpy v0.2.4. *Zenodo* **2014**.
- (34) Cheong, F. C.; Dreyfus, B. S. R.; Amato-Grill, J.; Xiao, K.; Dixon, L.; Grier, D. G. Flow Visualization and Flow Cytometry with Holographic Video Microscopy. *Opt. Express* **2009**, *17*, 13071–13079.

- (35) Holography and Light Scattering in Python — HoloPy 2.0.0 documentation <http://manoharan.seas.harvard.edu/holopy/> (accessed April 7, 2016)
- (36) Bohren, C. F.; Huffman, D. R. *Absorption and Scattering of Light by Small Particles*; Wiley-VCH: Germany, 1983.
- (37) Heinrich, V.; Wong, W. P.; Halvorsen, K.; Evans, E. Imaging Biomolecular Interactions by Fast Three-Dimensional Tracking of Laser-Confined Carrier Particles. *Langmuir* **2008**, *24*, 1194–1203.
- (38) Thompson, R. E.; Larson, D. R.; Webb, W. W. Precise Nanometer Localization Analysis for Individual Fluorescent Probes. *Biophys. J.* **2002**, *82*, 2775–2783.
- (39) Inamdar, M. M.; Gelbart, W. M.; Phillips, R. Dynamics of DNA Ejection from Bacteriophage. *Biophys. J.* **2006**, *91*, 411–420.
- (40) Gabashvili, I. S.; Grosberg, A. Y. Dynamics of Double Stranded DNA Reptation from Bacteriophage. *J. Biomol. Struct. Dyn.* **1992**, *9*, 911–920.
- (41) Petrov, A. S.; Harvey, S. C. Role of DNA–DNA Interactions on the Structure and Thermodynamics of Bacteriophages Lambda and P4. *J. Struct. Biol.* **2011**, *174*, 137–146.
- (42) Petrov, A. S.; Douglas, S. S.; Harvey, S. C. Effects of Pulling Forces, Osmotic Pressure, Condensing Agents and Viscosity on the Thermodynamics and Kinetics of DNA Ejection from Bacteriophages to Bacterial Cells: A Computational Study. *J. Phys. Condens. Matter* **2013**, *25*, 115101.
- (43) Marenduzzo, D.; Orlandini, E.; Stasiak, A.; Sumners, D. W.; Tubiana, L.; Micheletti, C. DNA–DNA Interactions in Bacteriophage Capsids Are Responsible for the Observed DNA Knotting. *Proc. Natl. Acad. Sci.* **2009**, *106*, 22269–22274.
- (44) Marenduzzo, D.; Micheletti, C.; Orlandini, E.; Sumners, D. W. Topological Friction Strongly Affects Viral DNA Ejection. *Proc. Natl. Acad. Sci.* **2013**, *110*, 20081–20086.
- (45) García, L. R.; Molineux, I. J. Rate of Translocation of Bacteriophage T7 DNA across the Membranes of Escherichia Coli. *J. Bacteriol.* **1995**, *177*, 4066–4076.
- (46) São-José, C.; de Frutos, M.; Raspaud, E.; Santos, M. A.; Tavares, P. Pressure Built by DNA Packing Inside Virions: Enough to Drive DNA Ejection in Vitro, Largely Insufficient for Delivery into the Bacterial Cytoplasm. *J. Mol. Biol.* **2007**, *374*, 346–355.
- (47) Knobler, C. M.; Gelbart, W. M. Physical Chemistry of DNA Viruses. *Annu. Rev. Phys. Chem.* **2009**, *60*, 367–383.
- (48) Jin, Y.; Sdao, S. M.; Dover, J. A.; Porcek, N. B.; Knobler, C. M.; Gelbart, W. M.; Parent, K. N. Bacteriophage P22 Ejects All of Its Internal Proteins before Its Genome. *Virology* **2015**, *485*, 128–134.
- (49) Löf, D.; Schillén, K.; Jönsson, B.; Evilevitch, A. Forces Controlling the Rate of DNA Ejection from Phage λ . *J. Mol. Biol.* **2007**, *368*, 55–65.

- (50) Lof, D.; Schillén, K.; Jönsson, B.; Evilevitch, A. Dynamic and Static Light Scattering Analysis of DNA Ejection from the Phage λ . *Phys. Rev. E* **2007**, *76*, 011914.
- (51) Leforestier, A.; Brasilès, S.; de Frutos, M.; Raspaud, E.; Letellier, L.; Tavares, P.; Livolant, F. Bacteriophage T5 DNA Ejection under Pressure. *J. Mol. Biol.* **2008**, *384*, 730–739.
- (52) Leforestier, A.; Livolant, F. The Bacteriophage Genome Undergoes a Succession of Intracapsid Phase Transitions upon DNA Ejection. *J. Mol. Biol.* **2010**, *396*, 384–395.
- (53) Leforestier, A. Polymorphism of DNA Conformation inside the Bacteriophage Capsid. *J. Biol. Phys.* **2013**, *39*, 201–213.
- (54) De Frutos, M.; Leforestier, A.; Livolant, F. Relationship between the Genome Packing in the Bacteriophage Capsid and the Kinetics of Dna Ejection. *Biophys. Rev. Lett.* **2013**, *09*, 81–104.
- (55) Keller, N.; del Toro, D.; Grimes, S.; Jardine, P. J.; Smith, D. E. Repulsive DNA-DNA Interactions Accelerate Viral DNA Packaging in Phage Phi29. *Phys. Rev. Lett.* **2014**, *112*, 248101.
- (56) Berndsen, Z. T.; Keller, N.; Grimes, S.; Jardine, P. J.; Smith, D. E. Nonequilibrium Dynamics and Ultraslow Relaxation of Confined DNA during Viral Packaging. *Proc. Natl. Acad. Sci.* **2014**, *111*, 8345–8350.
- (57) Jin, Y.; Knobler, C. M.; Gelbart, W. M. Controlling the Extent of Viral Genome Release by a Combination of Osmotic Stress and Polyvalent Cations. *Phys. Rev. E* **2015**, *92*, 022708.

Supporting Information

In Figure S1A we show line scans of the normalized holograms of the full and empty phages from Figure 5A in the main text. We show a horizontal and a vertical line scan of each hologram because the holograms are asymmetric owing to the slight tilt of the illumination beam. Additionally, we generate a hologram of the DNA in the capsid by dividing the hologram of a phage just before ejection by its hologram just after ejection. The ejecting phage we use to generate this hologram is the phage that produced the green curve in Figure 5D of the main text. This particular phage is chosen for comparison because the focal plane of the microscope during this ejection is most similar to the focal plane used when recording the full and empty phage holograms. Line scans of this DNA hologram are shown in Figure S1A along with those of the full and empty phages.

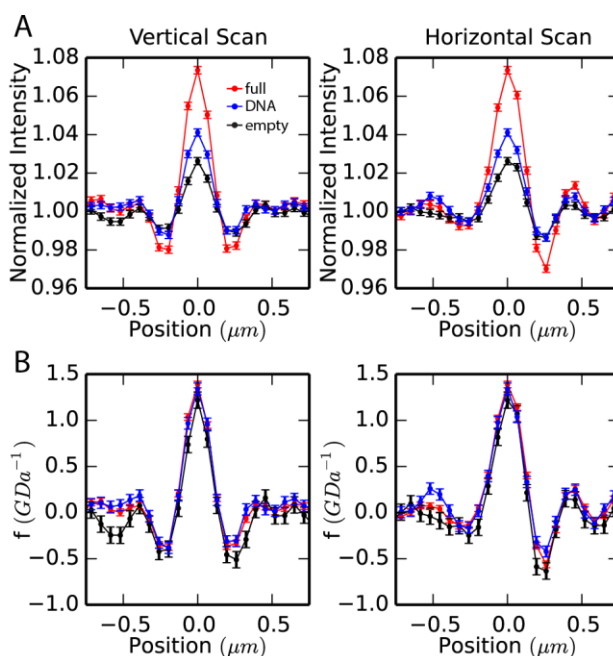


Figure S1: Vertical (left) and horizontal (right) line scans of holograms. A 10-frame time average was used for each hologram. Error bars represent the root mean square intensity of shot noise. Line scans of a full phage are plotted in red, line scans of an empty phage are plotted in black, and line scans of the DNA hologram are plotted in blue. **A:** Line scans of normalized holograms. **B:** Line scans of the hologram interference patterns scaled by the mass of the head of the phage.

In Figure S1B we show the line scans from Figure S1A scaled by the mass of each phage head. For the full and empty phages the scaled line scans were calculated by subtracting off the background and dividing by the mass of the phage head,

$$f_{f,e} = \frac{(H_{f,e} - 1)}{m_{f,e}}.$$

Here $f_{f,e}$ is the interference pattern from the full (f) or empty (e) phage normalized by the phage head mass, $H_{f,e}$ is the hologram of full or empty phage divided by an image of the reference beam, and $m_{f,e}$ is the phage head mass ($m_f = 54$ MDa and $m_e = 22$ MDa). When calculating the scaled line scans for the DNA hologram it is necessary to include the contribution of the empty phage;

$$f_{DNA} = \frac{(H_{DNA} - 1)}{m_f - m_e H_{DNA}}.$$

Here H_{DNA} is the hologram of a phage just before ejecting its DNA divided by the hologram of the same phage just after it has ejected its DNA.

The scaled line scans are quite similar to each other, particularly for the central fringes. Based on our hologram model for Rayleigh scatterers given in Equation (1) of the main text, we expect the interference patterns of different scatterers to be equivalent after scaling each by its total polarizability. The fact that the line scans of the different phage holograms overlap when scaled by the phage head mass supports our optical model of phage λ as a Rayleigh scatterer and suggests that the total polarizability is proportional to the mass of the head of the phage. Moreover, the excellent overlap between the central fringes of all 3 scaled interference patterns supports our choice to use the normalized central fringe intensity as a measure of the DNA content of phages during ejection. The agreement of the scaled fringe pattern from the DNA hologram with those of the empty and full phages also indicates that ejected DNA does not significantly contribute to the hologram after ejection.

Descriptions of Supporting Videos:

S1.avi:

Holographic video of a lambda phage in TNM buffer without detergent. The phage is bound to a coverslip that was cleaned by Pyrolysis. The video is recorded at 100 Hz with a 1 ms exposure time and plays at 10 Hz. The scale bar shows 360 nm. The phage tail is bound securely to the coverslip but the phage head is subject to thermal motion so the hologram intensity varies from frame to frame and the hologram is blurred.

S2.avi:

Holographic video of a lambda phage in TNM buffer without detergent. The phage is bound to a coverslip functionalized with APTES. The video is recorded at 10 Hz with a 28 ms exposure time and plays at 10 Hz. The scale bar shows 360 nm. The red line indicates the tracked position of the phage head. The phage head translates across the coverslip due to thermal motion.

S3.avi:

Holographic video of a lambda phage in TNM buffer containing 1% oPOE detergent. The phage is bound to a coverslip functionalized with APTES. The video is recorded at 100 Hz with a 6.5 ms exposure time and plays at 100 Hz. The scale bar shows 360 nm. The red line indicates the tracked position of the phage head. The phage translates across the coverslip due to thermal motion. For the last

15 seconds of the video the end of the phage tail is stuck securely in place and the head is confined to the perimeter of a 180-nm radius circle.

S4.avi:

Holographic video of a lambda phage in TNM buffer without detergent. The phage is bound to a coverslip functionalized with PEG and APTES. The video is recorded at 10 Hz with a 28 ms exposure time and plays at 10 Hz. The scale bar shows 360 nm. The red line indicates the tracked position of the phage head. The phage translates slightly across the coverslip due to thermal motion but is essentially fixed in place.

S5.avi:

Holographic video of a lambda phage in TNM buffer containing 1% oPOE detergent. The phage is bound to a coverslip functionalized with APTES. The video is recorded at 100 Hz with a 6.5 ms exposure time and plays at 100 Hz. The scale bar shows 360 nm. The red line indicates the tracked position of the phage head. The phage head translates across the coverslip due to thermal motion, but the end of the phage tail is stuck securely in place so the head is confined to the perimeter of a 180-nm radius circle .

S6.avi:

Holographic video (bottom) and tracked position (top) of a lambda phage in TNM buffer containing 1% oPOE detergent. The phage is bound to a coverslip functionalized with APTES. The video is recorded at 100 Hz with a 6.5 ms exposure time and plays at 100 Hz. The scale bar shows 360 nm. The track is offset from the holograms so that the fringe pattern can be clearly seen when the phage head leaves the coverslip. The track is black when the phage head is on the surface and red when it is above the surface. The phage head translates across the coverslip due to thermal motion and stands up on its tail.